Magnetic field effects on exciton and biexciton states in CuBr

J. C. Merle, A. Bivas,* C. Wecker, and B. Hönerlage
Laboratoire de Spectroscopie et d'Optique du Corps Solide,
Associé au Centre National de la Recherche Scientifique No. 232,
Université Louis Pasteur,
5 rue de l'Université, 67000 Strasbourg, France
(Received 29 September 1982)

In CuBr the polariton dispersion $E(\vec{Q},\vec{H})$ in the presence of a magnetic field $\vec{H}$ is dissymmetric with respect to $\vec{Q}$ and $\vec{H}$, $\vec{Q}$ denoting the polariton wave vector. We study this dissymmetry using hyper-Raman scattering techniques in the presence of a static magnetic field which is varied between -70 and 70 kG in a given configuration. The experimental results are quantitatively explained, considering $\vec{Q}$ and $\vec{H}$-linear terms in the exciton Hamiltonian. The effective g values and the C_Q-linear interaction term are determined with a good accuracy and an upper limit of the anisotropic exciton-mass parameters is established. Since biexcitons are involved in the scattering process, the influence of the magnetic field on their different states and on the selection rules of hyper-Raman scattering are studied. In agreement with our theoretical considerations, no decomposition of the biexciton ground state has been observed.

I. INTRODUCTION

Nonlinear spectroscopy has been of increasing interest these last years for the study of crystals, since the selection rules valid in multiphoton processes are different from those of linear spectroscopy. Therefore, complementary information on crystal properties may be achieved, provided that the level of excitation is kept reasonably low in order to exclude high-excitation phenomena such as renormalization effects. This is the case in hyper-Raman scattering, a process in which the transition probability is resonantly enhanced by biexcitons,[1,2] which have a giant oscillator strength.[3,4]

Concerning CuBr, experiments on hyper-Raman scattering have been performed and interpreted in terms of multicomponent excitonic polaritons.[5–8] Since this scattering process permits one to perform a spectroscopy in momentum space, the anisotropy and fine structure of the resulting dispersion relation could be well established. This study was only possible since the energy, symmetry, and dispersion of the different intermediate biexciton states were known from previous two-photon–absorption (TPA) measurements.[9–11]

Since the Hamiltonian, giving rise to the multicomponent polariton dispersion $E(\vec{Q})$, must be invariant under time reversal, the equality

$$E(\vec{Q})=E(-\vec{Q}) \tag{1}$$

holds for all wave vectors $\vec{Q}$ in the absence of magnetic fields $\vec{H}$. However, this relation is not necessarily valid at finite values of $\vec{Q}$, when an external magnetic field is applied. In this case, time-reversal invariance leads to[12]

$$E(\vec{Q},\vec{H})=E(-\vec{Q},-\vec{H})\neq E(-\vec{Q},\vec{H}) =E(\vec{Q},-\vec{H})\ . \tag{2}$$

An illustration of an effect of this kind due to important bilinear terms proportional to $\vec{Q}\wedge\vec{H}$ has first been given by Thomas and Hopfield when studying the reflectivity of the $2p$ (A) exciton in CdS.[13] In CuBr it should also be possible to establish relation (2) since $\vec{H}$- and $\vec{Q}$-linear interactions are both quite important.[5–8,14–17] However, in the exciton region various polariton branches interfere in a complicated way and therefore no observable effects could be obtained from reflectivity measurements.[18] They should also depend on the direction of the magnetic field with respect to crystallographic axes and to the direction of the exciting light beam. Since hyper-Raman scattering allows the excitation of polaritons with a well-defined wave vector, we have used this technique to demonstrate the importance of relation (2). We show that the observed energetic positions of hyper-Raman emission lines can be well explained by the combined effect of $\vec{Q}$- and $\vec{H}$-linear interactions. We can therefore determine the different g values of the conduction and of the valence band as well as the $\vec{Q}$-linear interaction term C_Q with good accuracy. In addition,

 ©1983 The American Physical Society

the combined effect of $\vec{H}$-linear and anisotropic $\vec{Q}$-quadratic interactions leads to a characteristic nonlinear variation of the energetic positions of hyper-Raman lines in a magnetic field. Since this variation was not observed in CuBr, we can give an upper limit of the anisotropic effective exciton mass parameters G_2 and G_3 as defined in Ref. 6.

In Fig. 1 the hyper-Raman scattering process[19,20] is given schematically in a backward scattering configuration. In this process, biexcitons are created virtually by the absorption of two polaritons with wave vector $\vec{q}_l$ and energy $\hbar\omega_l$. They recombine, obeying the laws of energy and momentum conservation:

$$2\hbar\omega_l = E_1(\vec{q}) + E_L(\vec{k}) , \qquad 2\vec{q}_l = \vec{q} + \vec{k} , \tag{3}$$

creating a longitudinal exciton with wave vector $\vec{k}$ and energy $E_L(\vec{k})$ and a polariton on the lower polariton branch $[\vec{q},E_1(\vec{q})]$. The latter polariton $[\vec{q},E_1(\vec{q})]$ is observed as a photon and gives rise to the hyper-Raman emission line R_L. The same process is possible for two polaritons as final states. The hyper-Raman lines change their spectral position if the frequency of the exciting laser is tuned. When, however, biexcitons are created resonantly, they may relax because of their finite lifetime before recombining radiatively. Energy and momentum conservations [Eq. (3)] would not be guaranteed in such a biexciton luminescence process, when considering only two incoming and two outgoing particles. Therefore, we first had to make sure that the emission lines observed corresponded to hyper-Raman emission lines (and not to biexciton luminescence) even when a magnetic field $\vec{H}$ is applied. Therefore, we first have to study the field dependence of the biexciton energies. In addition, selection rules of hyper-Raman scattering depend on the experimental configuration.[6] In order to attribute correctly the emission lines to the different polariton branches throughout the scattering process, we had to determine the selection rules in the presence of a magnetic field in a given direction.

In the next section, we study the biexciton system experimentally by two-photon absorption and theoretically by an invariant expansion of the Hamiltonian, describing the biexciton ground state in magnetic fields. In Sec. III, we present our experimental results, obtained by hyper-Raman scattering. We then study theoretically the dispersion of excitons and polaritons in magnetic fields and determine the relevant interaction parameters. Finally, we give some concluding remarks on the problem in Sec. IV.

II. BIEXCITONS IN A MAGNETIC FIELD

A. Experimental results of two-photon absorption

The experimental set up was quite similar to the one described in Refs. 9–11. We have studied cleaved CuBr platelets, immersed in pumped liquid helium at 1.6 K. They were grown by a vapor-phase transport method and their thickness was about 300 μm. They had parallel surfaces (110) and were properly oriented. As indicated in Fig. 2, they were positioned in the center of a superconducting coil giving rise to a reversible magnetic field $|\vec{H}|$ up to 70 kG.

Biexcitons are created by the simultaneous absorption of two photons from two different laser beams, both of which are linearly polarized. They are propagating along the [110] crystal axis but in opposite directions. This configuration is obtained when both beams excite opposite crystal surfaces.

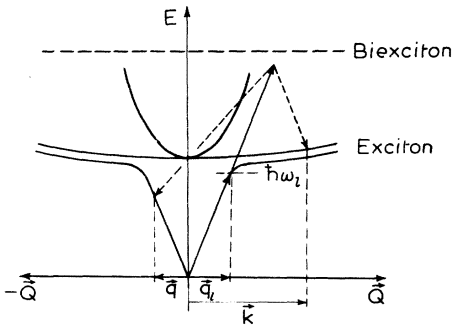

FIG. 1. Schematic representation of the hyper-Raman scattering. The details are discussed in the text.

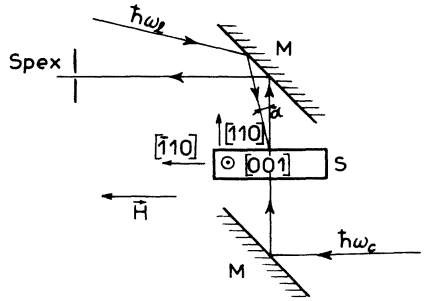

FIG. 2. Experimental configuration used in two-photon–absorption measurements. (M: mirror, S: sample, Spex: spectrometer, $\vec{H}$: magnetic field.) The laser excitation ($\hbar\omega_l$) and the continuum ($\hbar\omega_c$) propagate along the [110] crystal axis. The polarization vector $\vec{\epsilon}$ of both beams may be varied in the (110) plane.

In this "antiparallel" configuration,[10] biexcitons are created with a small wave vector ($\vec{K}\simeq 0$). One of the beams, having a small spectral width (0.35 meV) and high intensity, is a tunable "laser." The transmission through the crystal of the other, spectrally broad beam, called "continuum," is detected with and without excitation of the crystal by the laser. By these means, three different two-photon—absorption bands show up in the continuum. Their variation as functions of energy and polarization of the two beams with respect to the crystal axis allows us to identify the energy and symmetry of the final biexciton states, which are Γ_1, Γ_5, and Γ_3, respectively.[9–11] Their energies were given by[10]: $E_{\rm bi}(\Gamma_1)=5.9059$ eV, $E_{\rm Bi}(\Gamma_5)=5.9103$ eV, and $E_{\rm bi}(\Gamma_3)=5.9128$ eV, respectively.

In the presence of a magnetic field along the $[\bar{1}10]$ axis up to 70 kG, no modification of the intensity of the absorption dips is observed and the energies given above remain unchanged. In addition, no decomposition of the degenerate Γ_5 or Γ_3 levels is noticed. Only the absorption band corresponding to the Γ_5 biexciton level at vanishing field is slightly enlarged in our highest magnetic fields, i.e., the absorption band has 0.45 meV [full width at half maximum (FWHM)] at $H=0$ and 0.6 meV (FWHM) at $H=70$ kG if both beams are polarized along the $[\bar{1}10]$ direction. As we will see, this result can be fully understood theoretically.

B. Theoretical considerations

In CuBr the biexciton ground state is sixfold degenerated, having the symmetries Γ_1, Γ_3, and Γ_5 (Refs. 21 and 22) at the Γ point at vanishing symmetry-breaking effects. This degeneracy is split by different exchange interactions between the two holes, incorporated in the biexciton.[11,21] By two-photon—absorption experiments, this splitting as well as the biexciton dispersion could be determined.[9–11] In the latter experiment it turned out that the biexciton dispersion is fully understood from the exciton dispersive terms which were well known from hyper-Raman scattering.

In general, symmetry-breaking effects in the biexciton problem may be accounted for by constructing the effective Hamiltonian, acting in the 64-fold space of biexciton states, by means of an invariant expansion.[23,24] The Hamiltonian is built up from the subspaces of two electrons [indices $i=(1,3)$], each of which is two dimensional, and of two holes [indices $j=(2,4)$], each of which is four dimensional. $\vec{\sigma}^{(i)}=(\sigma_x^{(i)},\sigma_y^{(i)},\sigma_z^{(i)})$ and $1_e^{(i)}$ denote the electron-spin operator ($\sigma_x^{(i)},\sigma_y^{(i)},\sigma_z^{(i)}$ being the Pauli-spin matrices) and the two-dimensional unity matrix for the electron (i), respectively. Accordingly, the angular-momentum operators $\vec{J}^{(j)}=(J_x^{(j)},J_y^{(j)},J_z^{(j)})$ (with $J_x^{(j)}$, $J_y^{(j)}$, and $J_z^{(j)}$ being the angular-momentum matrices for $J=\frac{3}{2}$) build up the subspace for the two holes, $1_h^{(i)}$ denoting the four-dimensional unity matrix. The exchange interaction between the two holes may be diagonalized by using the symmetry-adapted biexciton wave functions given in Refs. 6 and 11, where the procedure is discussed in detail. Since in our two-photon—absorption experiments all biexcitons are excited in the antiparallel configuration, the biexciton wave vector $\vec{K}$ is almost equal to zero. Therefore we may neglect the symmetry breaking of the wave vector in our invariant expansion. Terms that mix $\vec{H}$ and $\vec{K}$ may be neglected because of the smallness of $\vec{K}$. Neglecting, furthermore, any dependence of the exchange interaction on the external magnetic field $\vec{H}=(H_x,H_y,H_z)$ and restricting ourselves to magnetic-field-dependent terms linear in $\vec{H}$, the perturbation in the biexciton Hamiltonian reads

$$H_{\rm bi}^H=\tfrac{1}{2}g_c\mu_B[(\vec{\sigma}^{(1)}\cdot\vec{H})\times 1_e^{(3)}\times 1_h^{(2)}\times 1_h^{(4)}+P_{13}]-2\kappa\mu_B[(\vec{J}^{(2)}\cdot\vec{H})\times 1_e^{(1)}\times 1_e^{(3)}\times 1_h^{(4)}+P_{24}]$$
$$-2q\mu_B[(H_xJ_x^{(2)^3}+\text{c.p.})\times 1_e^{(1)}\times 1_e^{(3)}\times 1_h^{(4)}+P_{24}]\,. \qquad (4)$$

In Eq. (4) c.p. denotes cyclic permutation and P_{ab} is an operator that exchanges the particles (a) and (b) in the foregoing expression. g_c, κ, and q are g values of conduction and valence bands, well known from the exciton problem,[14,15,23,24] and μ_B is Bohr's magneton. We may now construct the secular matrix corresponding to Eq. (4) and the different exchange interactions in the two-hole and two-electron representation as discussed in Refs. 6 and 11. We then transform the secular equation to the symmetry-adapted two-exciton wave functions in which exchange interactions are diagonalized. We then neglect the coupling of the sixfold biexciton ground state to the excited states (rotational states), which are probably much higher in energy. By this we obtain the six-dimensional secular matrix as given in Table I, describing the interacting biexciton states via a magnetic field. The corresponding dispersive terms using the same biexciton wave functions are given in Table II or Ref. 11. It is interesting to notice that the term proportional to the g factor of the conduction band g_c in Eq. (4) has no influence on

TABLE I. Secular matrix for interacting biexciton ground states in T_d symmetry in a magnetic field. Conjugated complex terms of the upper (lower) part have to be added to the lower (upper) part. The biexciton energies at vanishing magnetic field are given in Ref. 10 as follows: $E_{bi}(\Gamma_1)=5.9059$ eV, $E_{bi}(\Gamma_5)=5.9103$ eV, $E_{bi}(\Gamma_3)=5.9128$ eV, respectively. The biexciton wave functions $|\Gamma_l^j\rangle$ are defined in Table VIII of Ref. 6.

	$\|\Gamma_1\rangle$	$\|\Gamma_3^1\rangle$	$\|\Gamma_3^2\rangle$	$\|\Gamma_5^1\rangle$	$\|\Gamma_5^2\rangle$	$\|\Gamma_5^3\rangle$
$\langle\Gamma_1\|$	$E_{bi}(\Gamma_1)-E$	0	0	0	0	0
$\langle\Gamma_3^1\|$	0	$E_{bi}(\Gamma_3)-E$	0	0	$-2\sqrt{3}\kappa\mu_B H_x$	$-2\sqrt{3}\kappa\mu_B H_y$
$\langle\Gamma_3^2\|$	0	0	$E_{bi}(\Gamma_3)-E$	$+4\kappa\mu_B H_z$	$-2\kappa\mu_B H_x$	$+2\kappa\mu_B H_y$
$\langle\Gamma_5^1\|$	0	0	$+7q\mu_B H_z$	$E_{bi}(\Gamma_5)-E$	$-2i\kappa\mu_B H_y$	$-2i\kappa\mu_B H_x$
$\langle\Gamma_5^2\|$	0	$-\frac{7}{2}\sqrt{3}q\mu_B H_x$	$-\frac{7}{2}q\mu_B H_x$	$+\frac{13}{2}iq\mu_B H_y$	$E_{bi}(\Gamma_5)-E$	$+2i\kappa\mu_B H_z$
$\langle\Gamma_5^3\|$	0	$-\frac{7}{2}\sqrt{3}q\mu_B H_y$	$+\frac{7}{2}q\mu_B H_y$	$+\frac{13}{2}iq\mu_B H_x$	$-\frac{13}{2}iq\mu_B H_z$	$E_{bi}(\Gamma_5)-E$

the biexciton ground state. We now specialize to the experimental configuration, in which $-H_x=H_y=H/\sqrt{2}$ and $H_z=0$. We diagonalize the block of interacting biexciton states with Γ_5 symmetry separately and obtain the following eigenvalues:

$$E_{bi}^0(\Gamma_5,H)=E_{bi}(\Gamma_5)\,,$$
$$E_{bi}^{\pm1}(\Gamma_5,H)=E_{bi}(\Gamma_5)\pm\mu_B(2\kappa+\tfrac{13}{2}q)H\,. \tag{5}$$

The eigenfunctions corresponding to this block are given by

$$\psi_0(E_{bi}^0(\Gamma_5,H))=\frac{1}{\sqrt{2}}(|\Gamma_5^2\rangle+|\Gamma_5^3\rangle)\,,$$
$$\psi_{\pm1}(E_{bi}^{\pm1}(\Gamma_5,H))=\tfrac{1}{2}(\sqrt{2}i\,|\Gamma_5^1\rangle\pm|\Gamma_5^2\rangle \pm|\Gamma_5^3\rangle)\,, \tag{6}$$

where $|\Gamma_5^{(i)}\rangle$ are the biexciton Bloch functions defined in Ref. 6 and used as a basis in Table I.

Introducing $\kappa=-0.22$ and $q=0$ (from Sec. III C) in Eq. (5), we find that at our maximal magnetic field at 70 kG the splitting of the biexciton states is about 0.3 meV. In order to discuss the transition probability to the different biexciton states given in Eq. (5), we perform a coordinate transformation in the biexciton wave function of Ref. 6 using

$$|z\rangle'=\frac{1}{\sqrt{2}}(|x\rangle+|y\rangle)\,,$$
$$|y\rangle'=|z\rangle\,, \tag{7}$$
$$|x\rangle'=\frac{1}{\sqrt{2}}(-|x\rangle+|y\rangle)\,.$$

$|x\rangle$, $|y\rangle$, and $|z\rangle$ denote the Γ_5-exciton wave functions which are transforming like the vector components $[\vec{r}=(x,y,z)]$ defined in Ref. 6. In this new basis, selection rules are easily established in second-order perturbation theory. We then find the two-photon–absorption coefficient W to the different biexciton states with Γ_5 symmetry for photons propagating along the [110] direction to be proportional to

$$W(E_{bi}^0(\Gamma_5,H))\propto(\epsilon_l^{x'}\epsilon_c^{y'}+\epsilon_c^{x'}\epsilon_l^{y'})^2\,,$$
$$W(E_{bi}^{\pm1}(\Gamma_5,H))\propto\tfrac{1}{2}(\epsilon_l^{x'}\epsilon_c^{x'})^2\,. \tag{8}$$

In Eq. (8), $\epsilon_c^{x'},\epsilon_l^{y'}$ denote the components of the polarization vector of the laser (l) and continuum (c) in the $[\bar{1}10]$ and [001] direction, respectively.

From Eq. (8), we see that the transition to the biexciton states, which split to $\pm(2\kappa+\frac{13}{2}q)\mu_B H$ in a magnetic field, is equally allowed. Since the laser line has the halfwidth of about the splitting of the biexciton states in our maximal field H_M, we expect to observe an enlargement of the TPA dip in magnetic fields beyond 70 kG rather than a splitting in well-separated absorption dips. If the polarization of laser and continuum are along the [001] axis, no two-photon absorption is expected to be observed.

Concerning the Γ_3-biexciton states, they interact with each other only via a coupling to the biexciton states of Γ_5 symmetry. The coupling can be treated in perturbation theory. In this case, the energy shifts $\Delta E(\Gamma_3^{1,2},H)\lesssim 0.1$ meV for $H=70$ kG, which cannot be resolved experimentally. Finally the biexciton state with Γ_1 symmetry does not couple to the magnetic field at all. These results are consistent with our experimental findings discussed in Sec. II A.

In conclusion, we may state that the biexciton energies and the corresponding wave functions are not influenced by the magnetic field up to 70 kG at the Γ point. Since interactions depending simultaneously on $\vec{Q}$ and on $\vec{H}$ are higher-order perturbations,

this remains probably true at $\vec{Q}\neq 0$. It is confirmed by the fact that hyper-Raman emission and biexciton luminescence remain well separated even at our highest magnetic fields. As we will discuss in III B, a possible mixture of biexciton wave functions by a magnetic field does not alter the selection rules of hyper-Raman scattering when working with wave vectors $\vec{Q}\|[110]$ and $\vec{H}\|[\bar{1}10]$. Our results, therefore, show that biexcitons do not interfere with hyper-Raman data if the configuration given above is chosen.

III. EXCITONIC POLARITONS IN MAGNETIC FIELDS

A. Hyper-Raman scattering

Since hyper-Raman scattering has first been used to determine a complete set of parameters, describing the dispersion of excitonic polaritons in CuCl,[19,20] this method has been successfully applied to study more complicated structure such as CuBr,[5–8] CdS and ZnO,[25] or PbI_2.[26] As reviewed in Ref. 27, the properties of excitonic polaritons depend on the magnetic field, also. It is the aim of this section to derive the effective g values of the conduction- and valence-band electrons as well as to give further evidence of a $\vec{Q}$-linear interaction term.

In this experiment, the setup is essentially the same as discussed in Sec. II A (cf. Fig. 2). Only the light beam called continuum is suppressed. As is well known, the exciton ground state in CuBr is eightfold degenerate (with symmetries Γ_3, Γ_4, and Γ_5 at $Q=0$ and $H=0$). In the configuration indicated in Fig. 2, all these states couple to the electromagnetic radiation field, giving rise to ten polariton branches. Following Ref. 6, they are labeled A_1 to A_5 for the Σ_1 and B_1 to B_5 for the Σ_2 irreducible representation, respectively.

As was mentioned in the Introduction, biexcitons are virtually created by two-photon absorption from the laser beam, which excites the crystal at an angle of incidence of $\alpha=10°$. They may recombine to various couples of polaritons with wave vectors $\vec{k}^{(i)}$ and $\vec{q}^{(1)}$ due to the multicomponent structure of polaritons. Therefore, Eq. (3) must be changed to

$$2\vec{q}_l^{(1)}=\vec{k}^{(i)}+\vec{q}_i^{(1)}\,,$$
$$2E_1(\vec{q}_l^{(1)},\vec{H})=E_i(\vec{k}^{(i)},\vec{H})+E_1(\vec{q}_i^{(1)},\vec{H})\,, \tag{3'}$$

where $E_i(\vec{Q}^{(i)},\vec{H})$ denotes the energy of the polariton branch (i) at wave vector $\vec{Q}^{(i)}$ in the presence of the magnetic field $\vec{H}$. The final state, which is observed as a photon outside the crystal, is situated on the lower polariton branch (index 1). Since we are working in a backward scattering configuration, the wave vectors $\vec{k}^{(i)}$ of the different polaritons left behind are quite important, i.e., $|\vec{k}_i|\simeq 3|\vec{q}_l^{(1)}|$. These polaritons may belong to different branches (i), which gives rise to a fine structure of the hyper-Raman emission as it is discussed in Ref. 6. As indicated in Fig. 1, the wave vectors $\vec{q}_l^{(1)}$ and $\vec{q}_i^{(1)}$ are on the lower polariton branch in a region, where the group velocity is quite large. This part is not sensitively influenced by the magnetic field. Owing to momentum conservation [Eq. (3')], this statement holds also for $\vec{k}^{(i)}$. Moreover, a small variation of $\vec{k}^{(i)}$ does not affect $E_i(\vec{k}^{(i)},\vec{H})$, since the group velocity of the final states $\vec{k}^{(i)}$ is small for all branches. Therefore, hyper-Raman scattering enables us to determine from the conservation laws [Eq. (3')] the energies of different polariton states as function of $\vec{H}$, the wave vector $\vec{k}^{(i)}$ being constant, if the scattering configuration is kept fixed.

We have first tuned the laser frequency for various values of the magnetic field around the biexciton resonance in order to distinguish hyper-Raman lines from biexciton luminescence. As shown in Sec. II, the energy of the biexciton ground state does not depend on the magnetic field. Therefore, biexciton luminescence may always be avoided for a given excitation frequency and in the presence of a magnetic field.

For $\hbar\omega_l=2.9532$ eV, mainly biexcitons with Γ_1 symmetry [$E_{bi}(\Gamma_1 H)=5.9059$ eV from Ref. 10] are excited. For polarizations along the [001] direction (Σ_1), we observe a transition corresponding to the creation of a longitudinal exciton and a lower polariton [branches (A_4,A_1) of Ref. 6] as final states. This emission line (R_L) is not affected by the presence of the magnetic field. As shown in Fig. 3, we observe

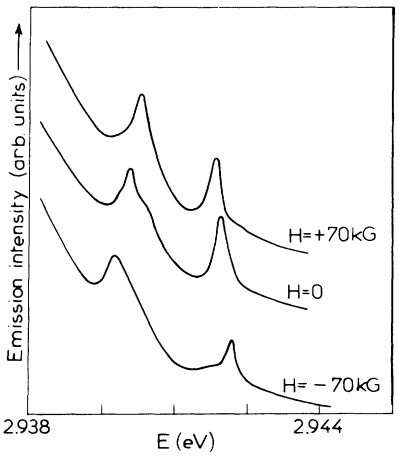

FIG. 3. Emission spectra of CuBr at different magnetic fields for the configuration of Fig. 2. The laser excitation is at $\hbar\omega_l=2.9532$ eV; exciting and observed photons are polarized along the $[\bar{1}10]$ direction.

two additional hyper-Raman lines at higher energies in the same polarization configuration. These lines change their spectral positions when the magnetic field is tuned.[28] The integrated intensity of the hyper-Raman emission lines remains independent of the magnetic field. They correspond to the R_T and R_t lines of Ref. 6. Similar spectra are observed for the polarization parallel to the [$\bar{1}$10] direction (Σ_2 irreducible representation).

As discussed above, we may calculate $E_i(\vec{k}^{(i)},\vec{H})$ from Eq. (3'), knowing the energy of the exciting polaritons and of the observed polaritons. Figure 4 shows the resulting energy variation of the final states as a function of the magnetic field $\vec{H}$ for the two polarizations discussed above. Their positions depend strongly on the magnetic field, reflecting the field dependence of the polariton dispersion which we will discuss in the next part.

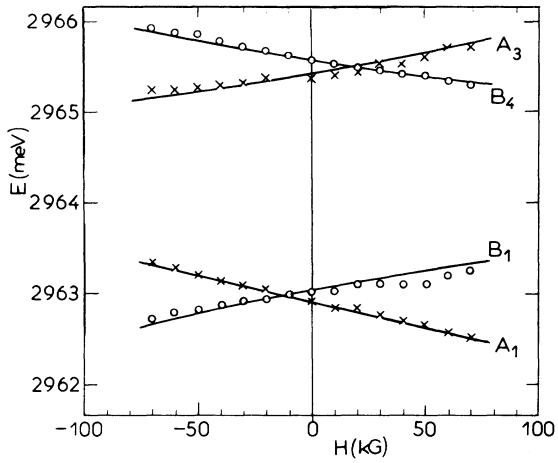

FIG. 4. Energy of the final states $E_i(\vec{k}^{(i)})$ in the hyper-Raman process as function of the magnetic field for the configuration of Fig. 2. The energy of the exciting photons is fixed at $\hbar\omega_l=2.9532$ eV. Crosses (×) correspond to emission lines polarized along the [001] direction, circles (○) to polarizations along [$\bar{1}$10]. Solid lines give the calculated positions of the branches A_1,B_1, and A_3,B_4.

B. Excitons and polaritons in magnetic fields

In CuBr the exciton ground state is eightfold degenerate at the Γ point, due to the fourfold degeneracy of the valence-band edge (Γ_8 symmetry) and the twofold degeneracy of the conduction band (Γ_6 symmetry). If we neglect all other states, the exciton Hamiltonian acting in this space may be constructed from an invariant expansion in function of the electron-spin operator $\sigma=(\sigma_x,\sigma_y,\sigma_z)$ (σ_i being the Pauli matrices for spin-$\frac{1}{2}$ particles) and the angular-momentum operator for $J=\frac{3}{2}$ [$\vec{J}=(J_x,J_y,J_z)$] as defined in Sec. II and Ref. 6. In the presence of magnetic fields, the Hamiltonian reads as follows:

$$
\begin{aligned}
H=&\Delta_0 1_e\times 1_h+\Delta_1\vec{\sigma}\cdot\vec{J}+G_1Q^2 1_e\times 1_h+C_Q[Q_x\{J_x,J_y^2-J_z^2\}+\text{c.p.}]\times 1_e\\
&+G_2[Q_x^2(J_x^2-1/3J^2)+\text{c.p.}]\times 1_e+2G_3[Q_yQ_z\{J_y,J_z\}+\text{c.p.}]\times 1_e\\
&+\tfrac{1}{2}g_c\mu_B\vec{\sigma}\cdot\vec{H}\times 1_h-2\mu_B[\kappa\vec{J}\cdot\vec{H}+q(H_xJ_x^3+\text{c.p.})]\times 1_e\ . \qquad (9)
\end{aligned}
$$

Here c.p. stands for cyclic permutation and $\{A,B\}=(AB+BA)/2$. The first six terms in Eq. (9) are detailed in Ref. 6. We consider here only the spherical part of the exchange interaction (Δ_0,Δ_1), which decomposes the exciton ground state in Γ_5-singlet states and in triplet states, having the symmetries Γ_3 and Γ_4. All other exchange interaction terms and their variations, e.g., with the finite wave vector $\vec{Q}$, are neglected for simplicity. As discussed in Refs. 6 and 23, the solution of the Schrödinger equation related to Eq. (9) gives rise to an anisotropic dispersion of the 1s exciton ground state.

Concerning the interaction with the magnetic field, g_c is the effect g value of the conduction-band electrons, and κ and q that of the valence electrons in degenerate bands.[29] The diamagnetic terms are negligible[30] even for our maximal magnetic field $H_{\max}=70$ kG and are therefore not mentioned here nor is a possible variation of the exchange interaction as function of the magnetic field. The interaction introduced by Thomas and Hopfield[13] would correspond to an electric field proportional to $\vec{Q}\wedge\vec{H}$ and is important only if the exciton radius is large. Taking into account the results on electroreflectance in Ref. 31, we can conclude that these effects are not important in CuBr.

The interaction matrix corresponding to the Hamiltonian given in Eq. (9) is transformed to the symmetry-adapted exciton functions, which are the same as in Refs. 6 and 23. The resulting matrix is found in the upper part of Table IX of Ref. 23, with the following definitions:

$$P=H_x,\ Q=H_y,\ R=H_z\ ,$$

and

$$\begin{aligned} g_1&=-\tfrac{1}{4}(6\kappa+\tfrac{27}{2}q-g_c)\mu_B\ ,\\ g_2&=-\tfrac{1}{4}(2\kappa+\tfrac{1}{2}q+g_c)\mu_B\ ,\\ g_3&=-\tfrac{1}{4}(6\kappa+\tfrac{15}{2}q-g_c)\mu_B\ ,\\ g_4&=-\sqrt{3/4}(2\kappa+\tfrac{13}{2}q+g_c)\mu_B\ ,\\ g_5&=-\tfrac{1}{4}(10\kappa+\tfrac{41}{2}q+g_c)\mu_B\ . \end{aligned} \tag{10}$$

This matrix is now specialized to our experimental configuration in which all wave vectors $\vec{Q}$ are taken along the [110] direction and the magnetic field parallel to the $[\bar{1}10]$ direction as indicated in Fig. 2. In this configuration the 8×8 matrix mentioned above may be partly diagonalized if using the wave functions for the high-symmetry case as given in Table IV of Ref. 6. The resulting two block matrices are given in Table II. Here Δ_{ST} denotes the singlet-triplet splitting and Δ_{LT} the longitudinal-transverse splitting at $\vec{Q}=0$ and $\vec{H}=0$. In this configuration, only the states labeled $|y\rangle'$ (irreducible representation Σ_1) and $|x\rangle'$ (Σ_2) are coupled to the electromagnetic light field which transforms like the same irreducible representation. We notice in Table II that exciton states belonging to different irreducible representations are not coupled by the magnetic field in our configuration. When partly diagonalizing the biexciton interaction matrix as described in Sec. II B by using the transformed biexciton states ψ_0 and $\psi_{\pm1}$, one can show that the selection rules of the hyper-Raman scattering for this configuration are the same as the ones for vanishing magnetic fields, which are given in Table X of Ref. 6. This means essentially that for a given polarization of the emitted light all final states belong to the same irreducible representation. This statement remains valid even if the biexciton wave functions are modified appreciably by the magnetic field (which is not the case here as discussed in Sec. II B) or if biexcitons with Γ_5 symmetry are excited resonantly. This is in agreement with the experimental results. It is important to notice in Table II that some matrix elements contain simultaneously terms proportional to $\vec{Q}$ and $\vec{H}$.

Therefore, the exciton dispersion is dissymmetric when, e.g., the wave vector is fixed and the direction of the magnetic field is inverted as indicated in relation (2). The terms proportional to Q^2 do not contribute to this effect.

Concerning the calculation of the polariton dispersion, we may proceed as discussed in Ref. 6,

TABLE II. Diagonal blocks of the exciton Hamiltonian for $\vec{Q}||[110]$ and $\vec{H}||[\bar{1}10]$. Only terms linear in $|\vec{H}|$ are considered. Complex conjugate terms of the lower (upper) part have to be added to the upper (lower) part. The zero of energy is that of the $(\Gamma_3+\Gamma_4)$-triplet state for $\vec{Q}=0$ and $\vec{H}=0$.

Σ_1	$\lvert1-\rangle'$	$\lvert2-\rangle'$	$\lvert y\rangle'$	$\lvert z\rangle'$
$\langle1-\rvert'$	$\left[G_1-\frac{1}{2}G_2\right]Q^2$	iHg_1		$i\sqrt{3}g_2H$
$\langle2-\rvert'$	$-i\frac{3}{4}C_QQ$	$\left[G_1+\frac{1}{4}G_2+\frac{3}{4}G_3\right]Q^2$	ig_4H	
$\langle y\rvert'$	$\frac{\sqrt{3}}{2}G_3Q^2$	$i\frac{\sqrt{3}}{2}C_QQ$	$\Delta_{ST}+\left[G_1+\frac{1}{2}G_2\right]Q^2$	$-ig_5H$
$\langle z\rvert'$	$i\frac{\sqrt{3}}{4}C_QQ$	$\frac{\sqrt{3}}{4}(G_2-G_3)Q^2$		$\Delta_{ST}+\Delta_{LT}+\left[G_1-\frac{1}{4}G_2-\frac{3}{4}G_3\right]Q^2$

Σ_2	$\lvert2+\rangle'$	$\lvert20\rangle'$	$\lvert1+\rangle'$	$\lvert x\rangle'$
$\langle2+\rvert'$	$\left[G_1+\frac{1}{4}G_2+\frac{3}{4}G_3\right]Q^2$		$\frac{1}{2}H(-3g_1+g_3)$	$\frac{1}{2}H(-\sqrt{3}g_2-g_4)$
$\langle20\rvert'$	$\frac{\sqrt{3}}{4}(G_2-G_3)Q^2$	$\left[G_1-\frac{1}{4}G_2-\frac{3}{4}G_3\right]Q^2$	$-\frac{\sqrt{3}}{2}H(g_1+g_3)$	$-\frac{1}{2}H(g_2-\sqrt{3}g_4)$
$\langle1+\rvert'$	$\frac{3}{8}C_QQ$	$\frac{\sqrt{3}}{8}C_QQ$	$\left[G_1+\frac{1}{4}G_2-\frac{3}{4}G_3\right]Q^2$	
$\langle x\rvert'$	$-\frac{5}{8}\sqrt{3}C_QQ$	$\frac{3}{8}C_QQ$	$-\frac{\sqrt{3}}{4}(G_2+G_3)Q^2$	$\Delta_{ST}+\left[G_1-\frac{1}{4}G_2+\frac{3}{4}G_3\right]Q^2$

16, or 32. Figures 5 and 6 give the dispersion of excitons and polaritons, propagating along the [110] direction, for polarizations along the [001] and [$\bar{1}$10] directions, respectively. In Figs. 5(a) and 6(a), the magnetic field is equal to zero. Figures 5(b) and 6(b) show the polariton dispersion in the presence of a magnetic field of 46 kG along the [$\bar{1}$10] direction. The combined effect of $\vec{Q}$-linear and $\vec{H}$-linear interactions leads to an appreciable dissymmetry of the dispersion, belonging to the two irreducible representations Σ_1 and Σ_2. We will now use this dispersion relation and the experimental results from Sec. III A in order to determine the effective g values and to discuss the dispersive terms in CuBr.

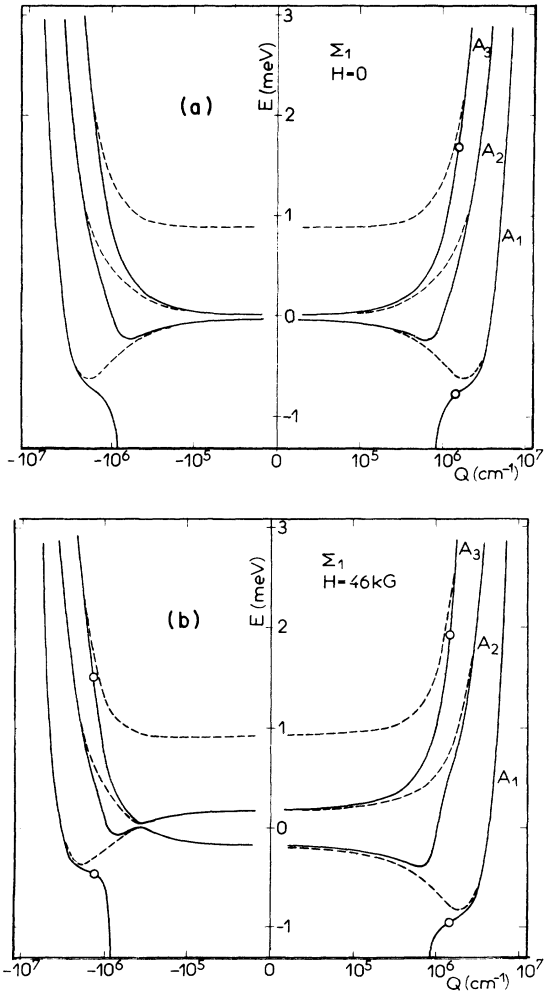

FIG. 5. Exciton (---) and polariton (—) dispersion in the [110] direction for polarization along the [001] crystal axis (Σ_1) for (a) $H=0$ and (b) $H=46$ kG with $\vec{H}\|[\bar{1}10]$. The parameters determining the dispersion are given in Eq. (11). An isotropic reduced mass $\mu=1.4m_0$ is also introduced.

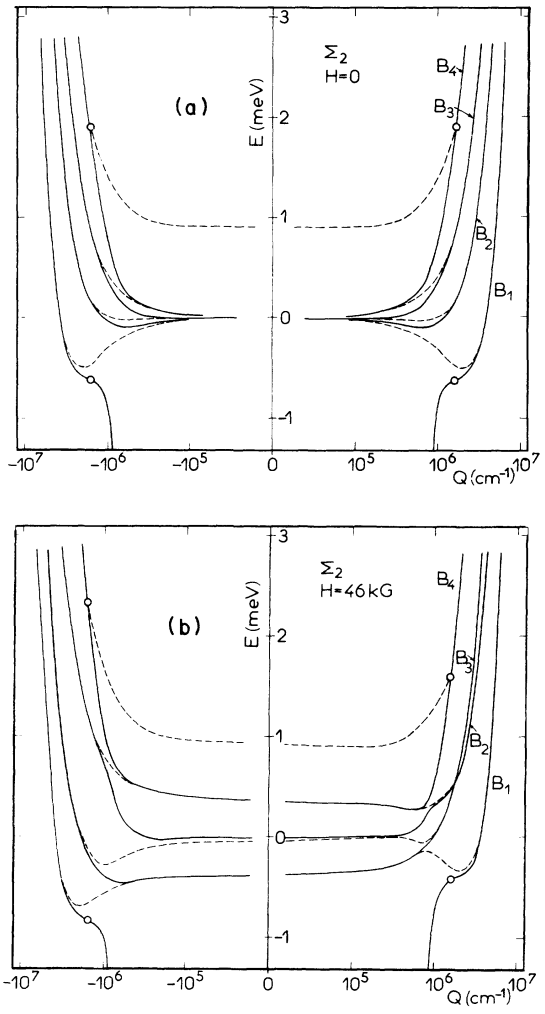

FIG. 6. Exciton (---) and polariton (—) dispersion in the [110] direction for polarization along the [$\bar{1}$10] crystal axis (Σ_2) for (a) $H=0$ and (b) $H=46$ kG with $\vec{H}\|[\bar{1}10]$. The parameters determining the dispersion are the same as in Fig. 5.

C. Discussion of the experimental results

In Figs. 5 and 6 we have labeled the different polariton branches from A_1 to A_3 and B_1 to B_4, respectively. [The longitudinal exciton (A_4) and the upper polariton branches (A_5,B_5) are not represented here because of the energy scale employed.] Concerning the R_L emission line (corresponding to final states on the branches A_1 and A_4, respectively, as shown in Fig. 1), we may further simplify the Σ_1 irreducible representation given in Table II. The state labeled $|z\rangle'$, which corresponds to the longitudinal exciton at $\vec{Q}=0$ and $\vec{H}=0$, is coupled to the other states only via matrix elements which are small

compared to Δ_{LT}. This explains why the A_4 state and therefore the R_L-emission line is not affected by the magnetic field as discussed in Sec. III A. Let us now simplify the problem further: Some of the parameters describing the polariton dispersion have already been studied previously (cf. Refs. 6, 33, and 34) and are well established. This is the case for the background dielectric constant $\epsilon_b=5.4$ and the longitudinal-transverse splitting $\Delta_{LT}=12.2$ meV. Since the excitation energy $\hbar\omega_l$ and the geometrical configuration remain fixed throughout the experiment, all wave vectors $\vec{k}^{(i)}$ have nearly the same value $|\vec{k}^{(i)}|\simeq 3|\vec{q}_l|$. (A more rigorous numerical calculation shows that $|\vec{k}^{(i)}|=1.44\times 10^6$ cm^{-1} can be used for all final states.) Therefore, the energies at $\vec{Q}=0$ and the isotropic (diagonal) effective exciton mass parameter G_1 cannot be determined separately. The same argument holds for a possible isotropic variation of the exchange Δ_{ST} with Q^2. Therefore, we will not bother about their absolute values but will determine only the splitting of singlet and triplet states $\tilde{\Delta}(Q)$ at the wave vector $|\vec{Q}|=1.44\times 10^6$ cm^{-1}. This does not introduce any restriction on the band parameters, which we will determine below.

In addition, we will neglect all possible variations of the exchange interaction with magnetic field or wave vector. This seems to be justified, since they are related to higher-order processes. In addition, we know from reflectivity measurements that q in Eqs. (4) and (9) must be very small since it does not give rise to any observable effect.[18] Therefore, we neglect q in the following discussion as well as interactions proportional to higher orders in $\vec{H}$.

With these approximations, the unknown parameters in the polariton dispersion resulting from Eq. (9) are $\tilde{\Delta}(k^{(i)})$, C_Q, G_2, G_3, g_c, and κ. These parameters are now adjusted in order to account for the energies of final states given in Fig. 4. The best result is obtained for

$$\begin{aligned}&\tilde{\Delta}(k^{(i)})=0.9\pm 0.1\ ,\\ &C_Q=69\pm 4\times 10^{-8}\ ,\\ &\kappa=-0.22\pm 0.05\ ,\\ &g_c=1.84\pm 0.1\end{aligned} \tag{11}$$

[where $\tilde{\Delta}(k^{(i)})$ is in units of meV, and C_Q is in units of meV cm]. In addition, the attribution of the final states to the hyper-Raman lines discussed above turns out to be unique.

Concerning G_2 and G_3,[35] their influence would result in a nonlinear dependence of the energies of the different branches as function of the magnetic field. This effect is shown in Fig. 7, where we tried to fit the energy difference ΔE of the branches A_1 and A_3 assuming $G_2=G_3=-0.2$. The best result is indicated by the solid line, but the overall agreement with this choice of G_2 and G_3 is quite poor. Since no nonlinear variation of ΔE with magnetic field is observed, we may give as an upper limit

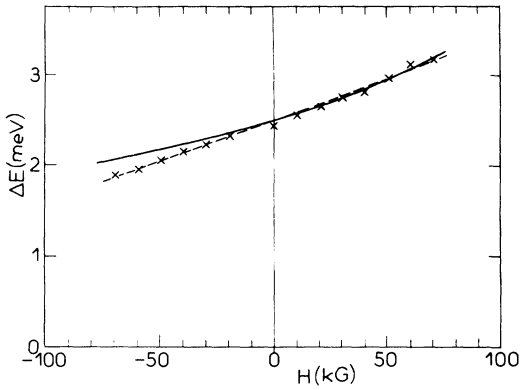

FIG. 7. Energy difference $\Delta E=E_{A_3}(k^{(i)})-E_{A_1}(k^{(i)})$ of the two branches. Crosses ($\times$) are experimental points. The dotted line (---) is calculated with the use of $G_2=G_3=0$ and the parameters of Eq. (11). The solid line (—) is calculated with the use of $G_2=G_3=-0.2$ and $\tilde{\Delta}(k^{(i)})=0.72$ meV, $C_Q=58\times 10^{-8}$ meV cm, $g_c=2.10$, $\kappa=-0.25$.

$$\begin{aligned}&|G_2|\le 0.2\\ &\text{and}\\ &|G_3|\le 0.2\ .\end{aligned} \tag{12}$$

Let us now discuss the influence of some exchange interactions which we have neglected up to now. As stated in Ref. 6, the exchange interaction may depend on the wave vector. The term which is probably most important reads $\delta_1\vec{\sigma}\cdot\vec{J}Q^2$. This effect would only influence the definition of $\tilde{\Delta}(Q)$ and we would obtain

$$\tilde{\Delta}(Q)=\Delta_{ST}-4\delta_1 Q^2\ . \tag{13}$$

On the other hand, the nonanalytic exchange interaction Δ_{LT} is expected to depend on the wave vector.[36] This dependence is, however, so small that it is not important at wave vectors $k^{(i)}=1.44\times 10^6$ cm^{-1} studied here. Concerning the anisotropic exchange parameters δ_2 and δ_3 of Ref. 6, they would result in similar nonlinear variations of ΔE in Fig. 7 as is the case for G_2 and G_3. The parameters given in Eq. (11) are in rather good agreement with hyper-Raman scattering results given in Refs. 5–8 and with reflectance measurements.[14,16–18,37] Concerning resonant Brillouin scattering in CuBr,[33,34] our values are compatible with the interpretation given in Ref. 38.

IV. CONCLUSION

We have studied excitonic polaritons and biexcitons in CuBr in magnetic fields up to 70 kG. Concerning the biexcitons, only an enlargement but no splitting of the biexciton states with Γ_5 symmetry (at vanishing symmetry-breaking effects) could be observed. This is due to the fact that the big g_c value of the conducting band, which is mainly responsible for the splitting and mixing of the exciton states in magnetic fields, does not influence the biexciton ground state. The other biexciton states are not essentially affected by the magnetic field.

For the geometric configuration given in Fig. 2, it turned out that the selection rules of hyper-Raman scattering do not depend on the strength of the magnetic field. Our analysis of observed shifts of hyper-Raman lines then enables us to determine exciton dispersive terms and effective g values in an original way. The simultaneous presence of Q- and H-liner interactions gives rise to a dissymmetry in the polariton dispersion, which is clearly established in this work. In addition, the attribution of the final states in previous hyper-Raman scattering experiments is verified and the magnitude of anisotropic mass parameters is discussed.

ACKNOWLEDGMENTS

The authors are grateful to Dr. J. B. Grun, Dr. R. J. Levy, and D. Q. H. Yu for their interest in our work and many stimulating discussions. We would like to thank Mrs. M. Joucla for the high-quality crystals of CuBr. Part of this work has been supported by the Ministre de l'Education Nationale of France.

---

*On leave at Gordon McKay Laboratory, Harvard University, Cambridge, Massachusetts.

[1]E. Hanamura, Solid State Commun. 12, 951 (1973).
[2]E. Doni, R. Girlanda, and G. Pasori-Parravicini, Solid State Commun. 17, 189 (1975).
[3]A. A. Gogolin, Fiz. Tverd. Tela. (Leningrad) 15, 2746 (1973) [Sov. Phys.—Solid State 15, 1824 (1974)].
[4]A. A. Gogolin and E. J. Rashba, Zh. Eksp. Teor. Fiz. Pis'ma Red. 17, 478 (1973).
[5]A. Bivas, Vu Duy Phach, B. Hönerlage, U. Rössler, and J. B. Grun, Phys. Rev. B 20, 3442 (1979).
[6]B. Hönerlage, U. Rössler, Vu Duy Phach, A. Bivas, and J. B. Grun, Phys. Rev. B 22, 797 (1980).
[7]Y. Nozue and M. Ueta, Solid State Commun. 36, 781 (1980).
[8]Y. Nozue, N. Miyahara, S. Takagi, and M. Ueta, Solid State Commun. 38, 1199 (1981).
[9]Vu Duy Phach and R. Levy, Solid State Commun. 29, 247 (1979).
[10]R. Levy, B. Hönerlage, and J. B. Grun, Phys. Rev. Lett. 44, 1355 (1980).
[11]B. Hönerlage, R. Levy, and J. B. Grun, Phys. Rev. B 24, 3211 (1981).
[12]V. M. Agranovich and V. L. Ginzburg, *Spatial Dispersion in Crystal Optics and the Theory of Excitons* (Interscience, London, 1966).
[13]D. G. Thomas and J. J. Hopfield, Phys. Rev. Lett. 5, 505 (1960); Phys. Rev. 124, 657 (1961).
[14]S. Suga, K. Cho, and M. Bettini, Phys. Rev. B 13, 943 (1976).
[15]C. Wecker, A. Daunois, J. L. Deiss, P. Fiorini, and J. C. Merle, Solid State Commun. 31, 649 (1979).
[16]P. Fiorini, J. C. Merle, and M. Simon, Phys. Rev. B 22, 4941 (1980).
[17]S. Suga, K. Cho, Y. Niji, J. C. Merle, and T. Sauder, Phys. Rev. B 22, 4931 (1980).
[18]J. C. Merle and C. Wecker (unpublished).
[19]B. Hönerlage, A. Bivas, and Vu Duy Phach, Phys. Rev. Lett. 41, 49 (1978).
[20]For recent review see J. B. Grun, in Proceedings of the 15th International Conference on the Physics of Semiconductors, Kyoto, 1980 [J. Phys. Soc. Jpn. 49, Suppl. A, 563 (1980)].
[21]E. Hanamura, J. Phys. Soc. Jpn. 39, 1506 (1975).
[22]C. Comte, Opt. Commun. 14, 79 (1975).
[23]K. Cho, Phys. Rev. B 14, 4463 (1976).
[24]G. L. Bir and G. E. Pikus, *Symmetry and Strain-Induced Effects in Semiconductors* (Wiley, New York, 1974).
[25]G. Blattner, G. Kurtze, G. Schmieder, and C. Klingshirn, Phys. Rev. B 25, 7413 (1982).
[26]Q. H. Yu, R. Levy, and B. Hönerlage, J. Lumin. 24/25, 417 (1981).
[27]J. Bimberg, in *Festkörperprobleme*, Vol. 19 of *Advances in Solid State Physics*, edited by J. Treusch (Vieweg, Braunschweig, 1979), p. 195.
[28]G. Kurtze, W. Maier, K. Kempf, G. Schmieder, H. Schrey, C. Klingshirn, B. Hönerlage, and U. Rössler, in Proceedings of the 15th International Conference on the Physics of Semiconductors, Kyoto, 1980 [J. Phys. Soc. Jpn. 49, Suppl. A, 559 (1980)].
[29]J. M. Luttinger, Phys. Rev. 102, 1030 (1956).
[30]S. Nikitine, J. Ringeissen, M. Certier, C. Wecker, S. Lewonczuk, J. C. Merle, and C. Jung, in *Proceedings of the 10th International Conference on the Physics of Semiconductors, Cambridge, Mass., 1970*, edited by S. P. Keller, J. C. Hensel, and F. Stern (United States Atomic Energy Commission, Division of Technical Information Extension, Oak Ridge, Tennessee, 1970), p. 196.
[31]J. L. Deiss and A. Daunois (private communication).
[32]K. Cho, Solid State Commun. 27, 305 (1978).

[33]Y. Oka and Vu Duy Phach, in Proceedings of the 15th International Conference on the Physics of Semiconductors, Kyoto, 1980 [J. Phys. Soc. Jpn. 49, Suppl. A, 547 (1980)].

[34]Vu Duy Phach, Y. Oka, and M. Cardona, Phys. Rev. B 24, 765 (1981).

[35]Using the perturbation theory approach of E. O. Kane, Phys. Rev. B 11, 3850 (1975), one would obtain $G_1=\hbar^2/2M_a$; $G_2=-\hbar^2\beta_h^2\gamma_2/m_0$; $G_3=-\hbar^2\beta_h^2\gamma_3/m_0$, with $\beta_h=[1+\gamma_1 m_e/m_0]^{-1}$, the Luttinger parameters $\gamma_1,\gamma_2,\gamma_3$ and M_a being a function tabulated by Kane.

[36]Y. Onodera, J. Phys. Soc. Jpn. 49, 1845 (1980).

[37]J. C. Merle, C. Wecker, and P. Fiorini, in *Proceedings of the 14th International Conference on the Physics of Semiconductors, Edinburgh, 1978,* edited by B. L. H. Wilson (IOP, Bristol, 1978), p. 1093.

[38]K. Cho and M. Yamane, Solid State Commun. 40, 121 (1981).